

## THE PHYSICAL AND DYNAMICAL CHARACTERISTICS OF THE ASTEROID 4940 POLENOV

E. Vchkova Bebekovska<sup>1</sup>, N. Todorović<sup>2</sup>, A. Kostov<sup>3</sup>, Z. Donchev<sup>3</sup>, G. Borisov<sup>4,3</sup>  
and G. Apostolovska<sup>1</sup>

<sup>1</sup>*Institute of Physics, Faculty of Science, Ss. Cyril and Methodius University,  
Arhimedova 3, 1000 Skopje, Republic of Macedonia*

E-mail: [elenavckova@gmail.com](mailto:elenavckova@gmail.com), [gordanaapostolovska@gmail.com](mailto:gordanaapostolovska@gmail.com)

<sup>2</sup>*Astronomical Observatory, Volgina 7, 11060 Belgrade, Serbia*

E-mail: [ntodorovic@aob.rs](mailto:ntodorovic@aob.rs)

<sup>3</sup>*Institute of Astronomy and National Astronomical Observatory, Bulgarian Academy of Sciences,  
Tsarigradsko Chaussee Blvd. 72, BG-1784, Sofia, Bulgaria*

E-mail: [akostov@astro.bas.bg](mailto:akostov@astro.bas.bg), [zahary.varna@gmail.com](mailto:zahary.varna@gmail.com), [gborisov@astro.bas.bg](mailto:gborisov@astro.bas.bg)

<sup>4</sup>*Armagh Observatory and Planetarium, College Hill, BT61 9DG Armagh, Northern Ireland, UK*

E-mail: [Galina.Borisov@Armagh.ac.uk](mailto:Galina.Borisov@Armagh.ac.uk)

(Received: October 1, 2020; Accepted: June 8, 2021)

**SUMMARY:** The asteroid (1986 QY4) 4940 Polenov is the first Solar system object whose 3D shape is determined using the observations from the newly built Astronomical Station Vidojevica (ASV). Here we present the results of photometric observations for Polenov, gathered from the ASV, and from the Bulgarian National Astronomical Observatory (BNAO) Rozhen, during 2014, 2019 and 2020 apparitions. Polenov is a 17.8 km object located in the outer part of the main belt and belongs to the asteroid family Themis. We have determined the lightcurves, the synodic period of  $4.161 \pm 0.001$  h, as well as the solution for the shape and spin axis. Using the lightcurve inversion method, the combination of our lightcurves and the sparse data from ATLAS-HKO and ATLAS-MLO, we also found the sidereal period, indicating a retrograde rotation of the asteroid, with two possible mirrored pole solutions. The ratio of the largest to smallest reflecting surface is about 1.4. In addition, we studied the dynamical properties of the asteroid and obtained a long stability time that exceeds 0.4 Gyrs.

**Key words.** Minor planets, asteroids: individual: 4940 Polenov – Techniques: photometric

### 1. INTRODUCTION

Asteroids are the smallest celestial bodies that are visible through the telescope. Despite their small dimensions, they played a key role in formation of our planetary system, and have also been involved in the

geological evolution of Earth. According to some researches, even the water on our planet, and the organic molecules (i.e. conditions for the origin of life), were delivered by asteroids (Morbidelli et al. 2000, O'Brien et al. 2014).

There are more than 900 000 currently known asteroids in the Solar system<sup>1</sup>, but only about 34000

---

© 2021 The Author(s). Published by Astronomical Observatory of Belgrade and Faculty of Mathematics, University of Belgrade. This open access article is distributed under CC BY-NC-ND 4.0 International licence.

---

<sup>1</sup>Taken from the AstDys data base <https://newton.spacedys.com/astdys/>.

have a known rotational period and about 2400 a known shape (data from September 2020). As a consequence of the huge number of collisions, most of the asteroids, especially the small ones, have irregular shapes; in mathematical modelling best approximated by triaxial ellipsoids (with semi-axis  $a, b, c$ ).

During their rotation, the size of the illuminated surface, as seen from the Earth, changes with time, repeating at regular intervals corresponding to the rotational period of the asteroid. The graph showing the change of the brightness with time is called *lightcurve* and represents the first step in further determination of physical parameters of an asteroid.

Here we will represent the photometric observations and some physical properties of the asteroid (1986 QY4) 4940 Polenov, discovered on 18<sup>th</sup> August 1986 from the Crimean Astrophysical Observatory at Nauchnyj<sup>2</sup>. The asteroid was named in honour of a notable Russian painter and humanist, Vasily Dmitrievich Polenov (1844-1927) (Schmadel 1997).

Polenov is a 17.8 km sized object (Masiero et al. 2011) located in the outer part of the main belt in the asteroid family Themis, at  $\sim 3.1$  AU. Its low albedo ( $\sim 0.08$ ) indicates a very dark surface meaning that it is most likely one of the carbonaceous C-type asteroids that inhabit the outer region of the main belt.

In the following sections, we give a brief description of the method used, data reduction, results of the observations, rotational properties and their uncertainties, and the shape model of Polenov. In addition, we analyse the dynamical stability of the asteroid for a time interval of 0.4 Gyrs.

We would like to add, furthermore, that Polenov is the first celestial body in the Solar system whose shape is determined from observations at the Astronomical station Vidojevica (ASV) in Serbia.

## 2. METHOD

The most common way to determine the rotation period, spin vector, and shape of an asteroid relies on the so-called *the lightcurve inversion method* (Kaasalainen and Torppa 2001, Kaasalainen et al. 2001). It is not always straightforward to find a unique solution for three-dimensional asteroid models since this method requires several dense lightcurves at different oppositions. Usually, tens of lightcurves are necessary for reconstruction of the shape model.

Recently, it was found that when there are not enough dense lightcurves, adding sparse photometric data could help to find a reasonable model solution. The idea of combining the dense lightcurve with the sparse data was firstly introduced by Kaasalainen (2004), and proven in practical work by Āurech et al. (2007). The sparse data include one or a few noisy points from each night of observation, making the determination of the period hardly possible. Using the sparse data can save a lot of observational time and also make use of fragmented/unfinished (due to bad weather conditions) photometric data sets.

<sup>2</sup>The discoverer was L. G. Karachkina who was credited by the Minor Planet Center for the discovery of 130 asteroids.

In the past few years, a lot of asteroid models have been determined using such shortened photometry. Āurech et al. (2018) gave a huge contribution in enlarging the DAMIT database<sup>3</sup>, containing asteroids with known models (Āurech et al. 2010). In their work, they have determined shape models of 908 asteroids, of which 662 were with unknown shape models while 264 had already determined models and were used for comparison. Combining the data from the GAIA DR2 mission and ground based telescopes, 762 more models were derived by Āurech et al. (2019a). Most of these models are based on combined dense lightcurves and sparse data but there are also models based on sparse data only. Some of the models are partially determined i.e. the solution for the spin axis latitude  $\beta$  is given, but the solution for the spin axis longitude  $\lambda$  is missing.

Having a large number of asteroids with a known shape model is useful in their further investigations. The spin vector distribution of asteroids can reveal whether their rotation is isotropic or anisotropic. At the moment, most of the larger asteroids have known spin vectors. But determining the spin vector for the smaller ones is an ongoing research, which will help in making conclusions, not just about the spin vector evolution, but also improve the theoretical and statistical modelling of collisional evolution of individual asteroid families (Hanuš et al. 2013, 2018) and the entire population of minor bodies in the Solar System (Vokrouhlický et al. 2017).

## 3. OBSERVATIONS AND DATA REDUCTION

In Table 1 we give the diameter ( $D$ ), the absolute magnitude ( $H$ ), albedo, and three orbital elements for 4940 Polenov: semi-major axis  $a$ , eccentricity  $e$  and inclination  $i$ . The data are taken from NASA's JPL/Horizons service<sup>4</sup>. The  $\sigma$  standard deviations are 0.111 for diameter and 0.010 for albedo. The error of the calculated albedo value, mostly caused by the uncertainty of the absolute magnitude (Pravec et al. 2012), has the highest value of 28% for objects with 10% errors in diameter and 0.2 mag uncertainty of the absolute magnitude (Masiero et al. 2021).

**Table 1:** Asteroid parameters for 4940 Polenov.

$D$ (km)	$H$ (mag)	Albedo	$a$ (AU)	$e$	$i$ ( $^{\circ}$ )
17.8	12.2	0.08	3.102	0.174	2.285

The photometric observations were performed during six nights at two observing sites. At the Bulgarian National Astronomical Observatory (BNAO) Rozhen the images were taken on 17<sup>th</sup> November

<sup>3</sup>Database of Asteroid Models from Inversion Techniques <https://astro.troja.mff.cuni.cz/projects/damit/>.

<sup>4</sup>Available at <https://ssd.jpl.nasa.gov/sbdb.cgi>

**Table 2:** Aspect data of 4940 Polenov for the six observing nights in 2014, 2019 and 2020 at the BNAO Rozhen and ASV.

Date (UT)	$r$ (AU)	$\Delta$ (AU)	Phase angle ( $\alpha$ ) ( $^\circ$ )	$\lambda_e$ ( $^\circ$ )	$\beta_e$ ( $^\circ$ )	Note
2014 Nov 17.97	2.6639	1.7163	7.57	76.14	-2.72	BNAO Rozhen 50/70cm Schmidt
2019 Sep 29.90	2.5862	1.5900	3.01	13.38	-3.54	AS Vidojevica ASA AZ1400
2019 Sep 30.99	2.5855	1.5882	2.58	13.16	-3.55	AS Vidojevica EQ60
2019 Oct 03.01	2.5843	1.5856	1.87	12.75	-3.56	BNAO Rozhen 60 cm Cassegrain
2020 Dec 18.99	2.9686	2.1682	12.96	130.10	-0.07	BNAO Rozhen 2 m RCC
2020 Dec 19.97	2.9702	2.1607	12.68	130.00	-0.06	BNAO Rozhen 2 m RCC

2014 by the 50/70 cm Schmidt telescope with an FLI PL16803 CCD camera, on 3<sup>th</sup> October 2019, by the 60 cm Cassegrain telescope with an FLI PL09000 CCD camera, and on 18<sup>th</sup> and 19<sup>th</sup> December 2020 by the 2 m RCC telescope using a 2-channel focal reducer Rozhen (FoReRo2) with the Andor iKon-L CCD. At the AS Vidojevica, the images were taken on 29<sup>th</sup> September 2019 by the 1.4 m "Milanković" telescope with the Andor iKon-L CCD, and on 30<sup>th</sup> September by the 60 cm "Nedeljković" telescope with an FLI PL230 CCD. All observations were done in the standard Johnson–Cousins R band. For differential aperture photometry we used CCDPHOT by [Buie \(1996\)](#). Lightcurve analyses (composite lightcurves, synodic rotational period and estimation of the amplitude of the lightcurve) were performed using MPO Canopus v10.7.7.0 ([Warner 2016](#)).

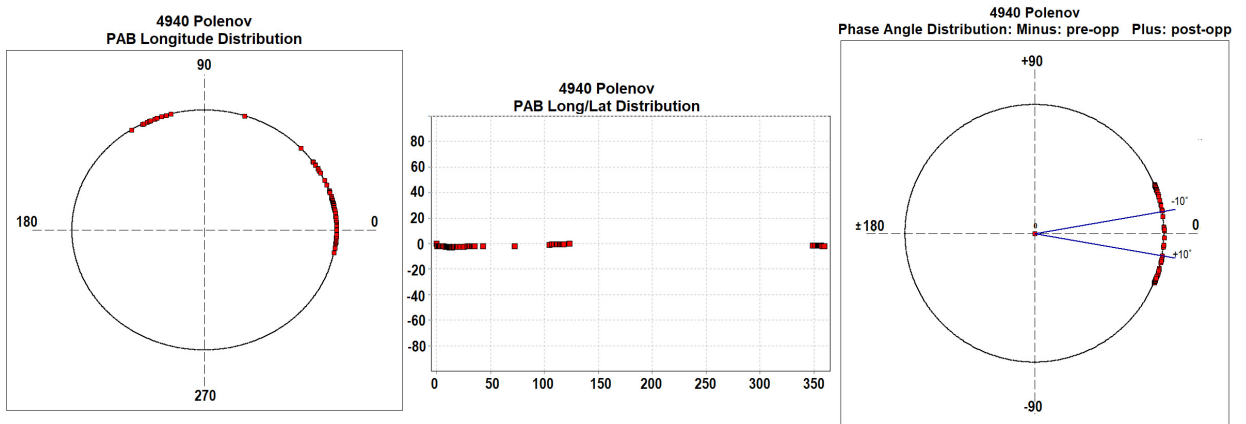
In Table 2 the aspect data of 4940 Polenov used for the observations are reported. The first column gives the date of the observation referring to the mid-time of the observed lightcurve. The following columns contain: the asteroid distance from the Sun ( $r$ ), distance from the Earth ( $\Delta$ ), the Sun-asteroid-observer angle (phase angle ( $\alpha$ )), the J2000.0 ecliptic longitude ( $\lambda_e$ ) and latitude ( $\beta_e$ ) of the asteroid, referred

to the time in the first column. The last column is a note on the source (observatory and telescope) used to acquire the images.

In the AstDys-2 database<sup>5</sup>, which we used for sparse data, most of the photometric data for 4940 Polenov are given with accuracy of 0.1 mags. Only in observations from 25<sup>th</sup> May 2019 to 4<sup>th</sup> November 2020 taken with the *Asteroid Terrestrial-impact Last Alert System* (ATLAS - observatory codes T05 and T08), we found data with photometric accuracy to 0.01 mag. For our calculations, we used photometry in an "orange" (o) band of 560-820 nm. Both observatories, T05 ATLAS-HKO and T08 ATLAS-MLO, are equipped with a 0.5m telescope. The ATLAS project is a robotic astronomical survey which covers the entire observable sky in one night up to brightness magnitude of 19 ([Tonry et al. 2018](#)). The ATLAS photometry has already been used to calculate spins and shape models of asteroids ([Durech et al. 2019b](#)).

In Fig. 1 the Phase Angle Bisector (PAB) longitude, PAB latitude, and phase angle distributions are presented for dense and sparse data used in the

<sup>5</sup><https://newton.spacedys.com/astdys/>


**Fig. 1:** Dense and sparse observations. Left: Distribution of PAB longitude; Center: Distribution of PAB longitude on PAB latitude; Right: Distribution of phase angle.

lightcurve inversion process. It is obvious that those observations, which are limited in three apparitions, could not give us a good aspect distribution coverage for a main-belt asteroid. Hence, to precise our solutions, we schedule more observations in different positions of this asteroid.

#### 4. RESULTS

Our first lightcurve for 4940 Polenov was obtained accidentally, namely on 17<sup>th</sup> November 2014 during the observations of the asteroid 967 Helionape. In the same field of view, beside our main target, during data reduction we noticed an asteroid which was identified as 4940 Polenov. Until that time, Polenov had no published lightcurve or rotation period. The field of view was observed for about three and a half hours, which covered one rotational period of our target, but unfortunately, it did not reveal the entire rotational period of Polenov. We observed the asteroid at the solar phase angle of  $7^{\circ}57'$  before its opposition on 4<sup>th</sup> December in the same year. The next opportunity to observe Polenov was in September and October 2019. It was observed three times in that period, on 29<sup>th</sup> and 30<sup>th</sup> September, and 3<sup>rd</sup> October, just before its opposition on 5<sup>th</sup> of October. The last set of our observations were done before the asteroid's opposition on 23<sup>rd</sup> January 2021, on 18<sup>th</sup> and 19<sup>th</sup> December 2020, when the solar phase angle was  $12^{\circ}9'$ , providing a better phase angle distribution.

The period analysis was done using Minor Planet Observer (MPO) Canopus, which incorporates the algorithm for Fourier Analysis of Light Curves (FALC) developed by [Harris et al. \(1989\)](#). The estimated rotational period  $4.161 \pm 0.001$  h has the smallest value

of the root mean square (RMS) error (Fig. 2) and the best correspondence to the observational points. The RMS errors for the two data sets have different sizes and amplitudes, but their smallest value and the best correspondence to the observational points matches at  $4.161 \pm 0.001$  h.

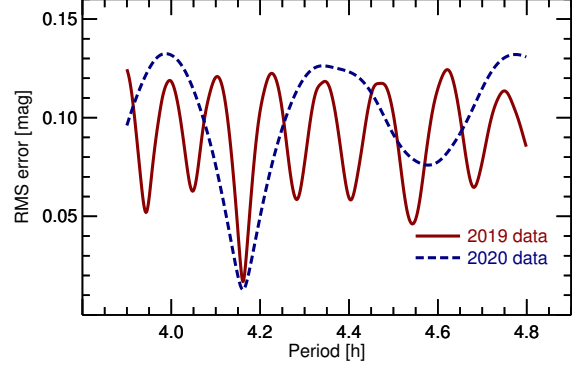


**Fig. 2:** The period spectrum for 4940 Polenov based on our observations from 2019 (marked with the solid red line) and 2020 (marked with the dashed blue line).

In Fig. 3 we present the lightcurve plotted by MPO Canopus that provides the best fit to  $4.161 \pm 0.001$  h as is using the 9<sup>th</sup> order fit Fourier analysis. The RMS scatter of the fit is 0.017 mag and the amplitude of the Fourier model curve is  $0.37 \pm 0.02$  mag. The x-axis rotational phase ranges from -0.05 to 1.05, and the magnitudes were normalized to the phase angle  $\alpha$  using the phase slope parameter  $G = 0.15$ .

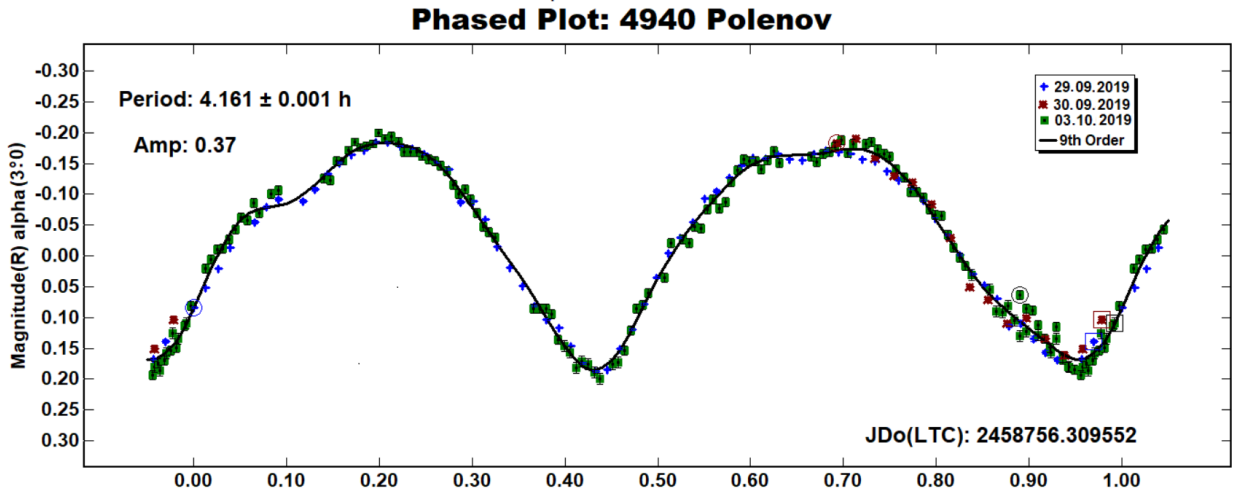


**Fig. 3:** The composite lightcurve of 4940 Polenov constructed from observations during three nights in 2019, where data from each night are marked with a different colour and symbol. The Fourier analysis of the order 9 gave the best fit corresponding to the rotational period  $4.161 \pm 0.001$  h with the amplitude of  $0.37 \pm 0.02$  mag.

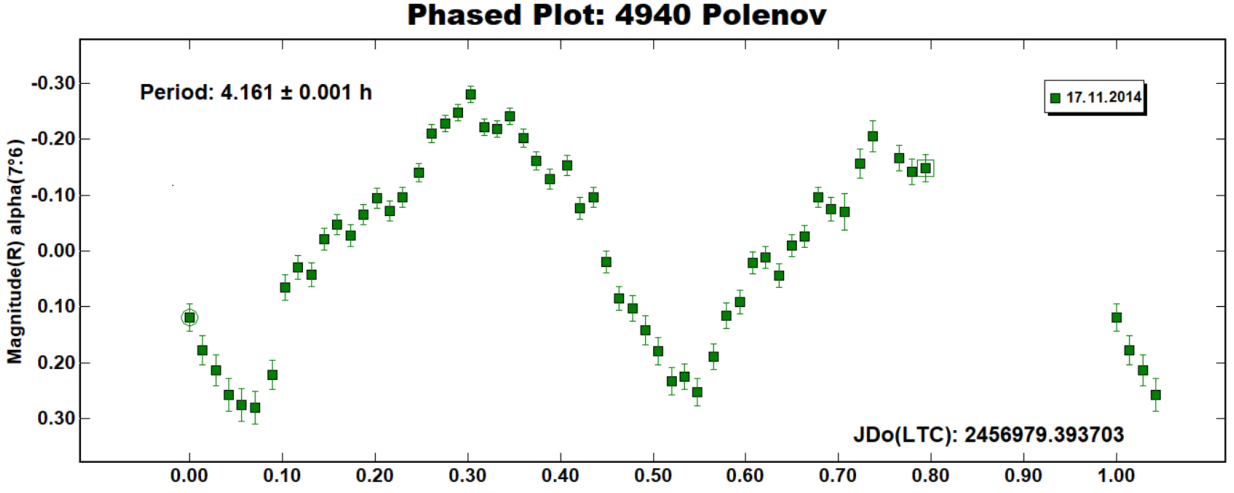


Fig. 4: The lightcurve of 4940 Polenov gathered from observations in 2014. Although not completely covered, it is constructed based on the afterwards calculated period of 4.161 h.

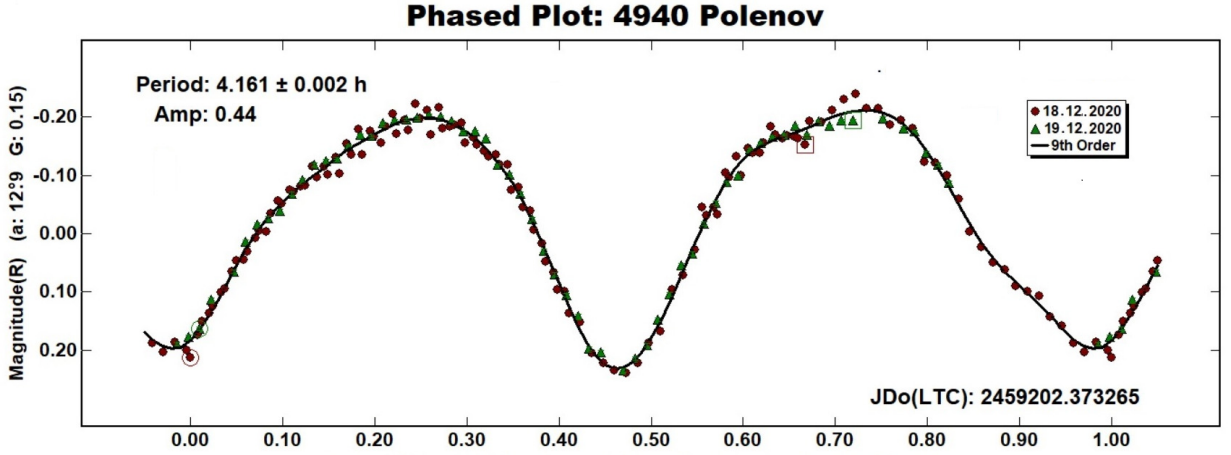


Fig. 5: The composite lightcurve of 4940 Polenov gathered from observations in 2020. The Fourier analysis of the order 9 gave the best fit corresponding to the rotational period  $4.161 \pm 0.001$  h with the amplitude of  $0.44 \pm 0.01$  mag.

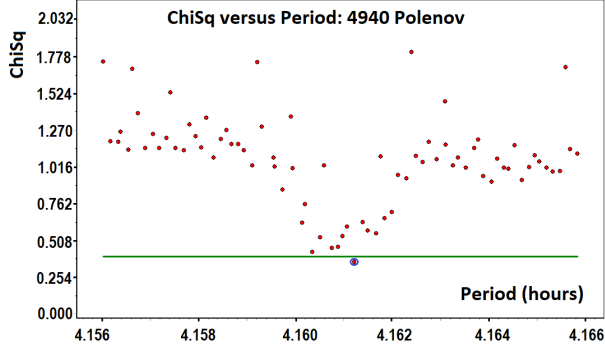
In Fig. 4 we show the lightcurve corresponding to the observations in 2014 when the period was not entirely covered, but the lightcurve was calculated on the basis of the rotation period of 4.161 h.

Fig. 5 shows the composite lightcurve gathered from observations in 2020 whose Fourier fit of the order 9 reveals a period of  $4.161 \pm 0.001$  h. The RMS scatter of the fit is 0.013 mag and amplitude of the Fourier model curve is  $0.44 \pm 0.01$  mag.

The shape of the two constructed composite lightcurves reveals two peaks with almost equal heights and sharp minima. From the fit of the lightcurve we can measure its amplitude and, using the empirical relation for the C-class asteroids  $A_0 = A/(1 + 0.015 \times \alpha)$  proposed by Zappala et al. (1990), we can calculate the so-called phase-corrected amplitude. Using its value we could calculate the ratio of the largest to smallest re-

flecting surface areas during the asteroid rotation as  $(a/c) = 10^{(0.4 \times A_0)}$ . In our case, we calculate  $(a/c) = 1.4$  for both lightcurves, which suggests a non-spherical form of the asteroid.

As already mentioned, we used the lightcurve inversion method for calculation the pole solution and derivation of the 3-dimensional shape model of the asteroid. The weighting factor for dense photometric data was set to 1.0, while for sparse photometric data it was set to one third of the dense data (Durech et al. 2009). The initial sidereal period search was made around our synodic period  $4.161 \pm 0.005$  h. A few number of solutions with 10% of the lowest  $\chi^2$  value were found, but a narrower period search found the most likely period (Fig. 6). The pole search checked 312 discrete, fixed pole positions but allowed the sidereal period to float around the most likely period. In



**Fig. 6:** A plot of  $\chi^2$  versus period.

Fig. 7 we can see that all solutions are with negative values for the pole latitude which firmly suggests the retrograde sense of asteroid rotation (usually denoted with  $R$ ). The dark blue regions have  $\chi^2$  values about 25% smaller than  $\chi^2$  values of the dark red regions.

From the pole search, we can recognize two roughly mirrored solutions with similar latitude that are separated by about  $180^\circ$  in longitude. A finer search, focused on these roughly possible pole positions, gave us more precise possible solutions. In Table 3 we give values of the estimated sidereal rotational period, sense of rotation, ecliptic coordinates of the two mirror solutions  $(\lambda, \beta)$ , as well as rough relative shape dimensions for Polenov. Assuming the asteroid as a triaxial ellipsoid with semi-axes  $a > b > c$ , that rotates around the shortest axis  $c = 1$ , we derived relative shape dimensions using data corresponding to the two poles, with  $(a/b)$  approximately equal 1.39 for both pole solutions, and a slightly more elongated shape in the  $(a/c)$  ratio with 1.55 and 1.46, respectively.

In order to obtain the uncertainties of our solutions for  $\lambda$  and  $\beta$  and the axis ratios we adopted the bootstrap approach described by Hanuš *et al.* (2015). For the purpose of bootstrapping we treated all the sparse data as a single (7th) lightcurve but with a lower weight as we did for the original solution. We randomly select seven lightcurves from our data set, which is equal to the number of lightcurves it contains. As a result, we can have some lightcurves multiple times and some missing in the new data set.

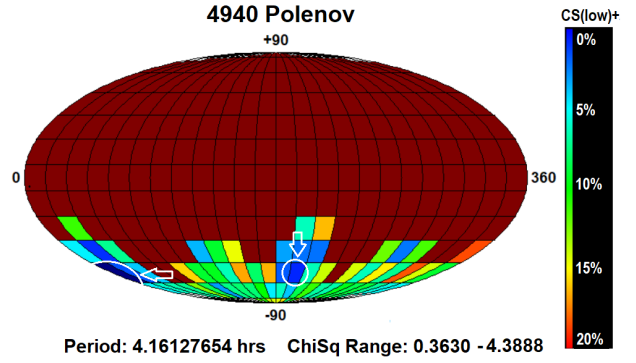


**Fig. 7:** Pole search distribution. The white arrows indicate the dark blue regions with smallest value of  $\chi^2$ .

We are doing this randomly 29 times and together with the original data we have 30 photometric data sets. We are using each of the new data sets to derive 30 solutions for the shape model by the lightcurve inversion. The rotational state is usually close to the original one as can be seen in Fig. 8. There we show the pole coordinates  $\lambda$  and  $\beta$  from the newly obtained shape models. All the solutions for  $\lambda$  and  $\beta$  fall within the intervals  $[0^\circ.6, 21^\circ.5]$  and  $[-86^\circ.5, -68^\circ.0]$ , respectively. The mirror solutions fall within  $[181^\circ.8, 204^\circ.5]$  and  $[-80^\circ.3, -56^\circ.0]$ , respectively. The mean values and their  $1-\sigma$  standard deviations are  $\bar{\lambda} = 9^\circ.2 \pm 6^\circ.4$  and  $\bar{\beta} = -78^\circ.1 \pm 5^\circ.1$ , and for the mirror solution  $\bar{\lambda}_m = 193^\circ.3 \pm 7^\circ.5$  and  $\bar{\beta}_m = -71^\circ.0 \pm 6^\circ.8$ , respectively. The original solutions fall within those  $1-\sigma$  intervals. As a part of the bootstrap procedure, we also computed the average axis ratios and their  $1-\sigma$  standard errors. They are as follows:  $\overline{(a/b)} = 1.34 \pm 0.11$  and  $\overline{(a/c)} = 1.62 \pm 0.25$ ,  $\overline{(b/c)} = 1.21 \pm 0.14$ , and for the mirror solution they are  $\overline{(a/b)}_m = 1.32 \pm 0.11$ ,  $\overline{(a/c)}_m = 1.59 \pm 0.20$  and  $\overline{(b/c)}_m = 1.22 \pm 0.11$ . The original solutions for the axes ratios also fall within those  $1-\sigma$  intervals as for the pole solution.

In Fig. 9 we give the obtained three-dimensional shape model of 4940 Polenov, where the four panels show the north and south pole views, and the two equatorial perspectives with rotational phases  $90^\circ$  apart, while the corresponding lightcurves are given in Fig. 10.

**Table 3:** In this table we give the sidereal period, sense of rotation where  $R$  stands for retrograde direction, the two pole coordinates  $(\lambda, \beta)$ , and the ratios of three semi-axes of the triaxial ellipsoid representing the shape model.

	Sidereal period (h)	Sense of rotation	Pole coordinates		$(a/b)$	$(a/c)$	$(b/c)$
			$\lambda(^{\circ})$	$\beta(^{\circ})$			
Pole1	$4.16128 \pm 0.00001$	$R$	6.8	-74.7	1.39	1.55	1.11
Pole2	$4.16128 \pm 0.00001$	$R$	191.6	-63.2	1.39	1.46	1.05

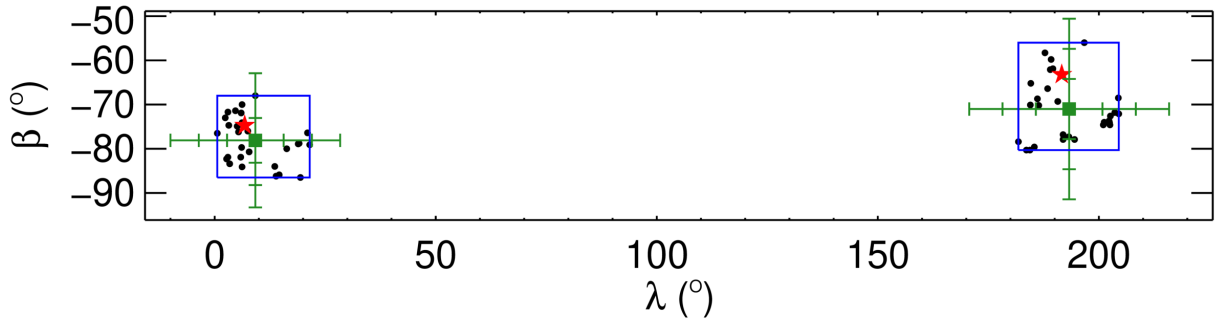


**Fig. 8:** The results of the pole solutions  $\lambda$  and  $\beta$  for each of the 30 photometric data sets obtained by the bootstrapping method. The blue rectangular regions show the range where all solutions fall within. The green squares show the average of all solutions and the green crosses with its tick-marks represent the 1, 2 and 3- $\sigma$  intervals. The original solutions are presented with red stars.

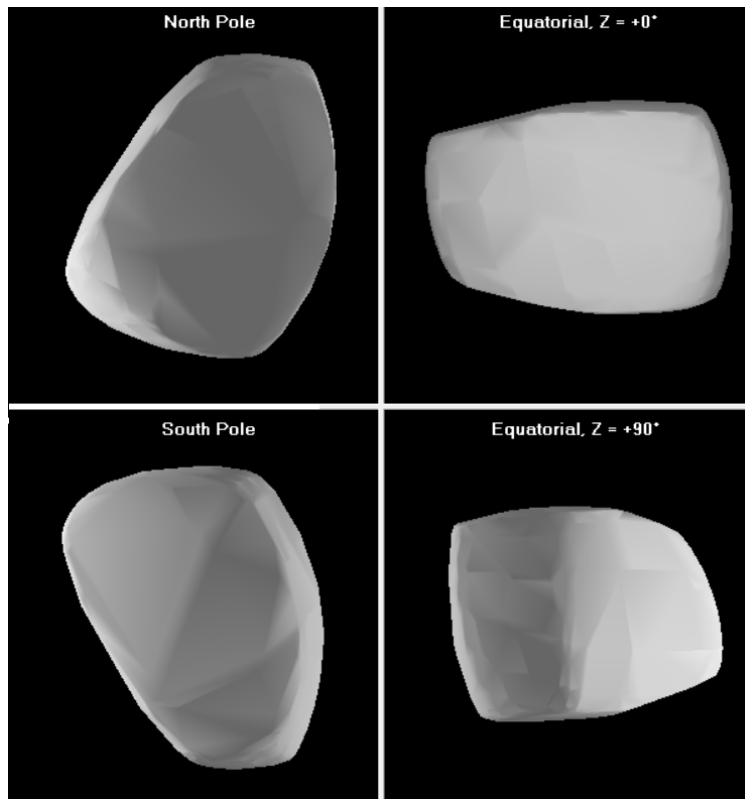


**Fig. 9:** The three-dimensional shape model of 4940 Polenov. The north and south pole view are given in two left panels, while the equatorial viewing and illumination geometry with rotational phases  $90^\circ$  apart, are given on the two right panels. The estimated aspect ratio of the longest to two shorter semi-axis is  $(a/b) \sim 1.4$  and  $(a/c) \sim 1.5$ . More accurate data are given in Table 3.

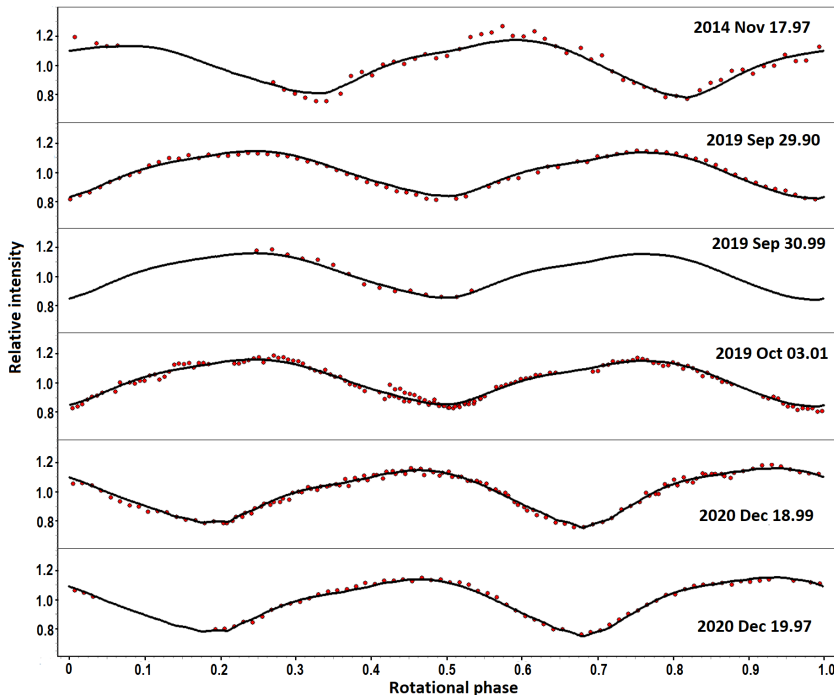


**Fig. 10:** The lightcurve points obtained from the dense observations (given in Table 2) and from the sparse data, superimposed over the lightcurves created by the model (solid line).

#### 4.1. The Stability Properties

In order to see the stability properties of Polenov, we have tracked its orbital evolution for more than 400 million years. The calculations are done in the ORBIT9 integrator<sup>6</sup> using a model with all planets from Venus to Neptune, while the mass of Mercury is added to the mass of the Sun and the corresponding barycentric correction is implemented to the initial conditions. The Yarkovsky effect was not considered. We registered the outputs every 250 yrs, filtering out the short periodic oscillations.

The calculations are performed in the osculating orbital elements starting with the epoch 30 September 2012 e.i. MJD 56200 (taken from the JPL/Horizons data base<sup>4</sup>). Initial values for the orbital elements were: semi major axis  $a = 3.1069$ , eccentricity  $e = 0.1703$ , inclination  $i = 2.2856$ , longitude of the node  $\Omega = 118.5010$ , argument of the pericenter  $\omega = 270.6249$ , and the mean anomaly  $M = 247.8699$ .

Fig 11 shows the evolution of Polenov’s semi-major axis ( $a$ ), where we can see that this is a very stable asteroid. Except for the very small local random variations, which are of the order  $\sim 10^{-4}$  AU, almost no other changes are notable. Similar behaviour is observed in the eccentricity ( $e$ ) and inclination ( $i$ ), not shown here, where the local random displace-

ments cover the intervals  $e \in [0.101, 0.17]$  and  $i \in [0^\circ.0014, 3^\circ.43]$ .

The asteroid is nested in between two high order mean motion resonances (MMR) with Jupiter<sup>7</sup>; between the 24J:11A at  $a \sim 3.0912$  AU (the place where asteroid makes 24 revolutions around the Sun while Jupiter makes 11) and 13J:6A at  $a \sim 3.1055$  AU (the place where asteroid makes 13 revolutions around the Sun while Jupiter makes 6).

In Fig. 11, except for the mentioned variations, a very small drift of the mean value of the semi-major axis is notable at  $t \sim 80 \times 10^6$  yrs, most likely caused by some high order resonance. We also notice that  $a_{\text{Polenov}}$  does not reach the values of  $a$  of the two neighbouring MMRs (24J:11A and 13J:6A). However, the resonant locations are not strictly fixed to one value of  $a$  but are capable for small local migrations along the semi-major axis (Malhotra and Zhang 2020).

We have checked the entries into the two MMRs by monitoring the corresponding resonant angles  $\sigma_{13J:6A}$  and  $\sigma_{24J:11A}$ , but we have not observed any indication of interaction with the two MMRs (for more details how to track entries into MMRs see e.g. Gallardo (2006), Todorović and Novaković (2015)), meaning that the small drift of  $a$  in Fig. 11 is most likely caused by some unidentified high order resonance.

<sup>6</sup>Available at <http://adams.dm.unipi.it/orbfit/>

<sup>7</sup>See Fig. 1 in Todorović (2020) for the resonant map of the Themis family.

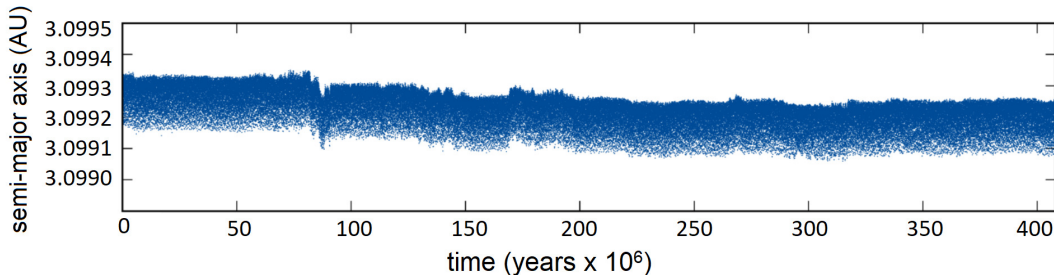


**Fig. 11:** Evolution of the semi-major axis  $a$  (AU) of the asteroid Polenov during the 400 Myrs integration. Except for the small local variations of the order of  $10^{-4}$ , slightly changing at  $t \sim 80 \times 10^6$ , no other changes in  $a$  are notable. The asteroid is located in between the two mean motion resonances with Jupiter,  $24A : 11J$  and  $13A : 6J$ , but it did not reach any of them in the observed time.

Recent studies in Hsieh et al. (2020) illustrated that Themis family members are capable to escape via some of the strongest resonances in the family and join the population of Jupiter family comets. Polenov, a quiet member of the family is not one of such escapers.

## 5. CONCLUSIONS

From our observations of the main-belt asteroid 4940 Polenov we estimated: its previously unknown rotational period to be  $4.161 \pm 0.001$  h, and its three-dimensional shape model. The constructed relative lightcurves from 2014, 2019 and 2020 have very similar shapes, revealing two peaks with almost equal heights and sharp minima. Calculations of the amplitude values gave us the approximate ratio of the largest to smallest reflecting surface areas during the asteroid rotation to be about 1.4.

Our pole coordinates calculations and obtained shape model are based on six dense lightcurves obtained over three oppositions (in 2014, 2019 and 2020) and sparse data from observations since May 2019 to November 2020 taken from AstDys-2<sup>5</sup>. Using the lightcurve inversion method we found that 4940 Polenov has a retrograde sense of rotation.

The determined solutions for the pole coordinates  $\lambda$  and  $\beta$  are  $6^\circ 8$  and  $-74^\circ 7$ , and  $191^\circ 6$  and  $-63^\circ 2$  for the mirror solution, respectively. The sidereal period  $4.16128 \pm 0.00001$  h was obtained in a simultaneous fit together with the pole coordinates and the shape. We analyse their uncertainties by applying the bootstrap approach described by Hanuš et al. (2015). The 95% confidence intervals of the bootstrap distributions are  $\lambda^{95\%} \in [0^\circ 6, 21^\circ 5]$  and  $\beta^{95\%} \in [-86^\circ 5, -68^\circ 0]$ , and for the mirror solutions they are  $\lambda_m^{95\%} \in [181^\circ 8, 204^\circ 5]$  and  $\beta_m^{95\%} \in [-80^\circ 3, -56^\circ 0]$ . We also want to emphasize that the original solutions fall within the  $1\text{-}\sigma$  intervals of average values of the bootstrapping distributions.

Let us mention furthermore that the limited coverage of the asteroid aspects by the data, and the fact that the retrograde spin pole being close to  $180$  degrees may gather some polar flattening and thus additional systematic errors. A detailed analysis of

such errors is beyond the scope of this paper and will be considered in more detail in our future work.

The calculated values of the ecliptic latitude of the 4940 Polenov pole are in favour of the obtained latitude distribution which shows that about half of the asteroids with a retrograde sense of rotation have latitudes in the interval  $[-53^\circ, -90^\circ]$ , and also fall within the latitude distribution for asteroids with diameters smaller than 30 km (Hanus̄ et al. 2011).

The lightcurve analysis of this asteroid gives us the opportunity to enlarge the database of asteroids (Warner et al. 2009) with a known period, but also with known physical properties, such as its shape. Additional data obtained in a longer time span of observation and in the wider range of aspect data could give more precise coordinates for the pole of the asteroid.

Numerical integration of the dynamical evolution of the asteroid have shown that Polenov is stable in time exceeding 400 million years.

*Acknowledgements* – Authors gratefully acknowledge the observing grant support from the Institute of Astronomy and Rozhen National Astronomical Observatory, Bulgarian Academy of Sciences. This research was partially supported by the Bulgarian National Science Fund grant DN 18/13-12.12.2017. The observations at AS Vidojevica and funding for N. T. were financed from the Ministry of Education, Science and Technological Development of the Republic of Serbia (contract no. 451-03-9/2021-14/200002). We are grateful to the anonymous referee who helped to shed more light on some of the results.

## REFERENCES

- Buie, M. W. 1996, in *Astronomical Society of the Pacific Conference Series*, Vol. 101, *Astronomical Data Analysis Software and Systems V*, ed. G. H. Jacoby and J. Barnes, 135
- Đurech, J., Scheirich, P., Kaasalainen, M., et al. 2007, in *IAU Symposium*, Vol. 236, *Near Earth Objects, our Celestial Neighbors: Opportunity and Risk*, ed. G. B. Valsecchi, D. Vokrouhlický, and A. Milani, 191–200

- Ďurech, J., Kaasalainen, M., Warner, B. D., et al. 2009, *A&A*, **493**, 291
- Ďurech, J., Sidorin, V. and Kaasalainen, M. 2010, *A&A*, **513**, A46
- Ďurech, J., Hanuš, J. and Alí-Lagoa, V. 2018, *A&A*, **617**, A57
- Ďurech, J., Hanuš, J. and Vančo, R. 2019a, *A&A*, **631**, A2
- Ďurech, J., Tonry, J., Erasmus, N., et al. 2019b, in EPSC-DPS Joint Meeting 2019, Vol. 2019, EPSC-DPS2019-404
- Gallardo, T. 2006, *Icar*, **184**, 29
- Hanuš, J., Ďurech, J., Brož, M., et al. 2011, *A&A*, **530**, A134
- Hanuš, J., Brož, M., Ďurech, J., et al. 2013, *A&A*, **559**, A134
- Hanuš, J., Delbo', M., Ďurech, J. and Alí-Lagoa, V. 2015, *Icar*, **256**, 101
- Hanuš, J., Delbo', M., Alí-Lagoa, V., et al. 2018, *Icar*, **299**, 84
- Harris, A. W., Young, J. W., Bowell, E., et al. 1989, *Icar*, **77**, 171
- Hsieh, H. H., Novaković, B., Walsh, K. J. and Schörghofer, N. 2020, *AJ*, **159**, 179
- Kaasalainen, M. 2004, *A&A*, **422**, L39
- Kaasalainen, M. and Torppa, J. 2001, *Icar*, **153**, 24
- Kaasalainen, M., Torppa, J. and Muinonen, K. 2001, *Icar*, **153**, 37
- Malhotra, R. and Zhang, N. 2020, *MNRAS*, **496**, 3152
- Masiero, J. R., Mainzer, A. K., Grav, T., et al. 2011, *ApJ*, **741**, 68
- Masiero, J. R., Wright, E. L. and Mainzer, A. K. 2021, *The Planetary Science Journal*, **2**, 32
- Morbidelli, A., Chambers, J., Lunine, J. I., et al. 2000, *M&PS*, **35**, 1309
- O'Brien, D. P., Walsh, K. J., Morbidelli, A., Raymond, S. N. and Mandell, A. M. 2014, *Icar*, **239**, 74
- Pravec, P., Harris, A. W., Kušnirák, P., Galád, A. and Hornoch, K. 2012, *Icar*, **221**, 365
- Schmadel, L. D. 1997, Dictionary of Minor Planet Names. Third, revised and enlarged edition (Springer-Verlag, Berlin, XIV+940 Seiten)
- Todorović, N. 2020, in IAU General Assembly, 17–18
- Todorović, N. and Novaković, B. 2015, *MNRAS*, **451**, 1637
- Tonry, J. L., Denneau, L., Heinze, A. N., et al. 2018, *PASP*, **130**, 064505
- Vokrouhlický, D., Bottke, W. F. and Nesvorný, D. 2017, *AJ*, **153**, 172
- Warner, B. D. 2016, MPO Canopus software, <http://www.MinorPlanetObserver.com>
- Warner, B. D., Harris, A. W. and Pravec, P. 2009, *Icar*, **202**, 134
- Zappala, V., Cellino, A., Barucci, A. M., Fulchignoni, M. and Lupishko, D. F. 1990, *A&A*, **231**, 548

**ФИЗИЧКЕ И ДИНАМИЧКЕ КАРАКТЕРИСТИКЕ  
АСТЕРОИДА 4940 ПОЛЕНОВ**

**E. Vchkova Bebekovska<sup>1</sup>, N. Todorović<sup>2</sup>, A. Kostov<sup>3</sup>, Z. Donchev<sup>3</sup>, G. Borisov<sup>4,3</sup>  
and G. Apostolovska<sup>1</sup>**

<sup>1</sup>*Institute of Physics, Faculty of Science, Ss. Cyril and Methodius University,  
Arhimedova 3, 1000 Skopje, Republic of Macedonia*

E-mail: *elenavchkova@gmail.com, gordanaapostolovska@gmail.com*

<sup>2</sup>*Astronomical Observatory, Volgina 7, 11060 Belgrade, Serbia*

E-mail: *ntodorovic@aob.rs*

<sup>3</sup>*Institute of Astronomy and National Astronomical Observatory, Bulgarian Academy of Sciences,  
Tsarigradsko Chaussee Blvd. 72, BG-1784, Sofia, Bulgaria*

E-mail: *akostov@astro.bas.bg, zahary.varna@gmail.com, gborisov@astro.bas.bg*

<sup>4</sup>*Armagh Observatory and Planetarium, College Hill, BT61 9DG Armagh, Northern Ireland, UK*

E-mail: *Galina.Borisov@Armagh.ac.uk*

УДК 523.44 POLENOV

*Оригинални научни рад*

Астероид 4940 Поленов (1986QU4) је први објекат Сунчевог система чији је тродимензионални облик одређен користећи посматрања са новоизграђене Астрономске станице Видојевица (АСВ). У изложеном раду дајемо резултате фотометријских посматрања Поленова, прикупљених са АСВ, као и са Бугарске националне астрономске опсерваторије (БНАО) Рожен у току три опозиције 2014, 2019. и 2020. године. Поленов је објекат величине 17.8 km и налази се у спољном делу главног астероидног појаса, у астероидној фамилији Темис. Одредили смо криве сјаја за овај објекат, његов синодички период од

$4.161 \pm 0.001$  часова, и дали решење за његов облик и положај оса ротације. Методом инверзије кривих сјаја, комбинацијом кривих сјаја и проређених *ATLAS-HKO* и *ATLAS-MLO* података, добијен је и сидерички период, показано је да астероид има ретроградну ротацију, и дата су два могућа огледалска решења за координате полова. Однос између највеће и најмање рефлектујуће површине је 1.4. Додатно је анализирана и динамика астероида, где је показано да је Поленов изразито стабилан астероид, са временом стабилности већим од 0.4 милијарде година.